

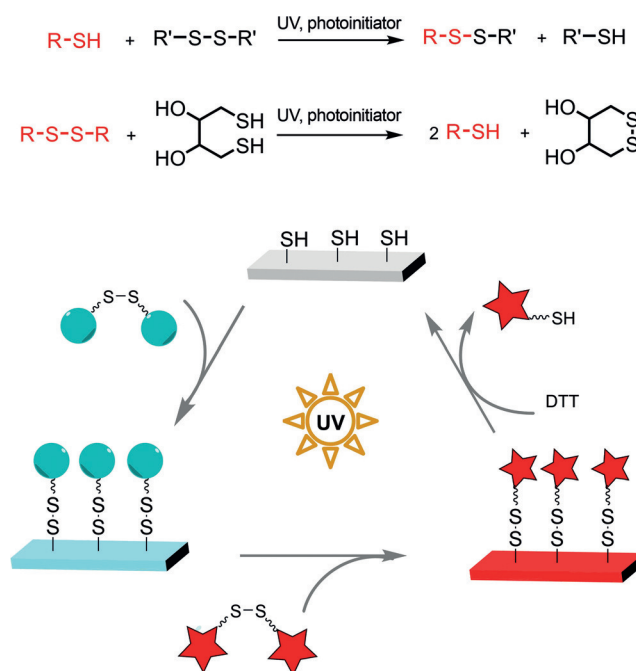
UV-Induced Disulfide Formation and Reduction for Dynamic Photopatterning

Lei Li, Wenqian Feng, Alexander Welle, and Pavel A. Levkin*

Abstract: UV-induced disulfide formation (UV-DF) and disulfide reduction (UV-DR) reactions for surface functionalization and dynamic photopatterning are presented. Both photochemical reactions allow for the spatially and temporally controlled, reversible transition between thiol- and disulfide-functionalized surfaces. The dynamic photopatterning strategy was demonstrated by the UV-induced attachment, exchange, and detachment on thiol-modified substrates.

Spatially resolved functionalization of surfaces is important in a variety of research fields ranging from microfluidics^[1] and electronics^[2] to biotechnology.^[3] In this context, photochemical reactions attracted attention, because they offer both spatial and temporal control of surface modification.^[4] To date, a variety of light-triggered reactions, for example, thiol-ene^[5]/yne,^[6] photoinitiated azide-yne,^[7] tetrazole-ene,^[8] tetrazole-thiol,^[9] and phototriggered Diels-Alder reactions,^[10] have been exploited for surface functionalization. However, the majority of the existing methods are restricted to irreversible surface functionalization because of the formation of relatively non-reactive covalent bonds. In contrast, reversible photochemical modifications provide more diverse possibilities for surface manipulation. These can be applied, for example, for dynamic tuning of interfacial properties, stimuli-responsive activation and deactivation of specific functions, or reversible attachment/detachment of functional moieties. To the best of our knowledge, only three examples of reversible phototriggered surface functionalization methods, based on the thiol-quinone methide reaction,^[11] the addition-fragmentation chain-transfer reaction of allyl sulfides with thiols,^[12] and the photodynamic disulfide exchange reaction (PDDE),^[13] have been reported. Herein, we demonstrate two photo-induced reactions that allow for spatially

and temporally controlled thiol-disulfide interconversions, namely UV-induced disulfide formation (UV-DF) and disulfide reduction (UV-DR) reactions. These reactions are used to demonstrate reversible UV-induced surface modification, patterning, and attachment as well as detachment of functional molecules (Scheme 1).



Scheme 1. Schemes of the UV-DF and UV-DR reactions (top). Reversible attachment, exchange, and detachment of disulfide-modified substrates by using the dynamic UV-DF, UV-DR, and PDDE photo-reactions (bottom).

[*] Dr. L. Li, W. Feng, Dr. P. A. Levkin
Institute of Toxicology and Genetics (ITG)
Karlsruhe Institute of Technology (KIT)
76021 Karlsruhe (Germany)
E-mail: levkin@kit.edu
Homepage: <http://www.levkingroup.com>

W. Feng
Organisch-Chemisches Institut
Ruprecht-Karls-Universität Heidelberg
69120 Heidelberg (Germany)

Dr. A. Welle
Institute of Functional Interfaces (IFG), KIT (Germany)

Dr. A. Welle
Karlsruhe Nano Micro Facility (KNMF) (Germany)

Supporting information and the ORCID identification number(s) for the author(s) of this article can be found under:
<http://dx.doi.org/10.1002/anie.201607276>.

Thiol-disulfide interconversion is well-documented to proceed through the thiolate-centered mechanism,^[14] however, it lacks the spatial control required for surface patterning. Recently, several works have demonstrated that disulfide exchange reactions can be performed by photoirradiation.^[13,15] Inspired by this process, we envisioned that thiol-disulfide exchange reactions could also be initiated by light through the thiol-centered mechanism. Apart from one example^[16] of using this strategy as a gelation reaction, the potential of the UV-DF and UV-DR for surface modification, to the best of our knowledge, has not been explored.

First, we explored the UV-DF for functionalizing a thiol-modified surface (Figure 1A). A porous polymeric film was used as the substrate to facilitate the monitoring of surface modification using static water contact angle (WCA) and

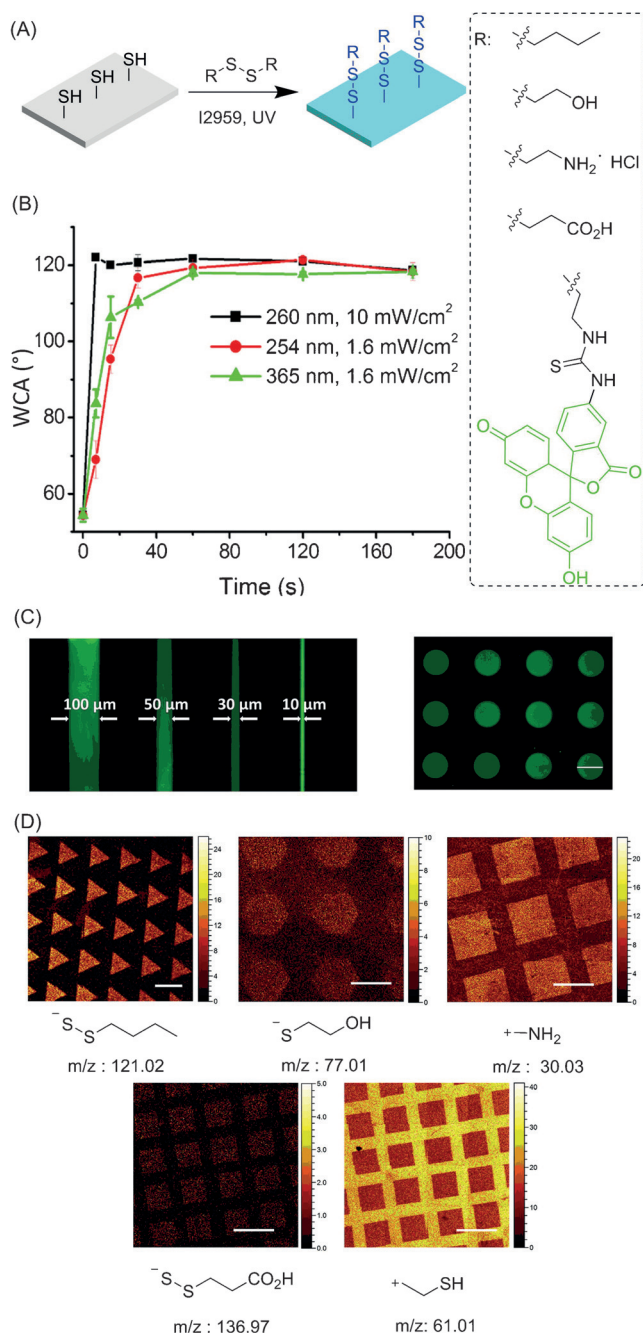


Figure 1. A) Representation of the UV-DF reaction on thiol-modified surfaces. B) Rate of surface modification by the UV-DF reaction in DMF. Static WCA on a thiol-functionalized surface after the UV-DF reaction with dibutyl disulfide as a function of irradiation time using different UV sources. C) Fluorescence microscopy images of a thiol-functionalized surface patterned with FITC-disulfide through different photomasks. Scale bar = 500 μm . D) ToF-SIMS images of a thiol-modified surface patterned with (from left to right) dibutyl disulfide, bis(2-hydroxyethyl) disulfide, cysteamine dihydrochloride, and bis(2-carboxyethyl) disulfide. The last image shows a ToF-SIMS image of intact thiol groups after patterning with bis(2-carboxyethyl) disulfide. Scale bars = 500 μm .

fluorescence measurements. The substrate was prepared through the esterification of a porous poly(hydroxyethyl methacrylate-*co*-ethylene dimethacrylate) film^[17] with bis(2-

carboxyethyl) disulfide (CDS) with subsequent reduction of the disulfides by 1,4-dithiothreitol (DTT) catalyzed by triethylamine (Supporting Information, Scheme S1). The thiol content on the surface, determined spectrophotometrically by titration with 2,2'-dipyridyl disulfide according to the literature procedure,^[18] was $1.94 \times 10^{-9} \text{ mol mm}^{-2}$. The obtained film was hydrophilic, with a static WCA of $54 \pm 2^\circ$.

To test the UV-DF reaction, dibutyl disulfide (BDS) was used as the model compound. The thiol-functionalized film was wetted with a solution of BDS (20 wt %) and the commercial photoinitiator I2959 (1 wt %) in DMF. After 2 min of UV irradiation (260 nm, 10 mW cm^{-2}), the static WCA increased from $54 \pm 2^\circ$ to $118 \pm 2^\circ$, demonstrating the successful immobilization of hydrophobic butyl groups. The conversion degree of thiol groups was determined to be 80 % (Supporting Information, Figure S11 and Table S2). To monitor the surface modification process, we measured the static WCA of the surface exposed to UV light for different irradiation times. As shown in Figure 1B, the static WCA increased to $118 \pm 2^\circ$ after only 7 s of irradiation and remained stable afterwards, demonstrating the fast reaction kinetics, which is important for creating patterns with high contrast and resolution. The UV-DF modifications are also efficient under UV irradiation both with lower light intensity (254 nm, 1.6 mW cm^{-2}) and at a longer wavelength (365 nm, 1.6 mW cm^{-2}), which shows promise for patterning UV-sensitive biomolecules.

This photochemical reaction allows for a spatially controlled disulfide attachment on thiol-modified surfaces. Figure 1C demonstrates sharp fluorescent patterns with features as small as 10 μm produced by photopatterning of FITC-disulfide on a thiol-functionalized surface. Considering the roughness and thickness (12.5 μm) of the polymeric surface used, this result is attributed to the fast kinetics of the UV-DF reaction. A wettability gradient on the thiol-functionalized surface was also prepared by surface modification with BDS using a moving photomask (Supporting Information, Figure S15).

The chemical compositions of the surfaces were characterized by time-of-flight secondary ion mass spectrometry (ToF-SIMS). As for the thiol-derivatized film patterned with BDS, Figure 1D shows the pattern of butyl moieties with a good resolution. We further evaluated this photopatterning with bis(2-hydroxyethyl) disulfide (HDS), cysteamine dihydrochloride (ADS), and CDS. The high-contrast patterns in Figure 1D demonstrate the good tolerance of this reaction towards hydroxy, amino, and carboxyl groups.

Next, we investigated the possibility of a UV-induced disulfide reduction to cleave previously grafted groups. It is well documented that disulfide bonds can be reduced by DTT through the thiolate-centered mechanism.^[14,19] Under UV light, the disulfide reduction will proceed through thiolate-centered and thiol-centered processes. To compare the rates of these two processes, we performed the model reaction of HDS (11 mM) with DTT (22 mM) in different solvents with or without the presence of a photoinitiator (I2959, 2.2 mM) and UV irradiation (254 nm, 1.6 mW cm^{-2}). The Supporting Information Figures S1–S4 and Table S1 show the ^1H NMR results under different conditions. In $[\text{D}_6]\text{DMSO}$, the con-

version of HDS under UV irradiation is 3.4-fold faster than that without UV irradiation; in CDCl_3 and $\text{D}_2\text{O}/\text{DCI}$ (0.72 wt % DCI), the reduction reaction only occurred under UV irradiation. These results imply that this reaction is dominated by the thiol-centered process in less polar solvents and/or acidic solutions.

These primary results prompted us to explore this UV-DR reaction on the surface. We tested the reduction of CED-modified films and determined spectrophotometrically the conversion of disulfides. The results are summarized in the Supporting Information, Table S2. In DMF, the conversion of disulfide was 34 % within 2 min of UV irradiation (260 nm, 10 mW cm^{-2}), almost ten-fold higher than that without UV irradiation. In CHCl_3 , 95 % of disulfides have been reduced after 5 min of UV irradiation, while the conversion is only 4.3 % without UV irradiation. This large difference in reaction rates is important for achieving temporal and spatial control for surface modification. We further characterized this UV-DR reaction on the hydrophobic DBS-modified surface using contact angle measurements. As shown in Figure 2B, the static WCA decreased from $118 \pm 2^\circ$ to $54 \pm 2^\circ$, which corresponds to the original thiol-modified surface, after 2 min of UV irradiation (260 nm, 10 mW cm^{-2}). This indicates that the hydrophobic butyl groups have been removed by the UV-DR reaction. In contrast, no change of the static WCA was detected after 2 min without UV irradiation, which is consistent with the observed slow kinetics of this reaction in organic solvents without any catalyst (Supporting Information, Table S1). Further study of the surface modification process shows that the UV-DR reaction is completed in less than 2 min and also proceeds effectively under 260 and 365 nm light (1.6 mW cm^{-2} , Figure 2B). The Supporting Information Figures S13 and S14 show that both UV-DF and UV-DR reactions proceed even without the photoinitiator at 254 nm, albeit slower than with the initiator.

To demonstrate the possibility for photopatterning using the UV-DR, the (FITC-disulfide)-functionalized film was subjected to UV irradiation (260 nm, 10 mW cm^{-2}) through a photomask in the presence of a solution of DTT (20 wt %) and I2959 (1 wt %) in CHCl_3 . Patterns with various shapes could be easily prepared by using different photomasks (Figure 2C). The photopatterning was also confirmed by the ToF-SIMS results of a BDS-functionalized film irradiated with UV through a photomask in the presence of DTT in CHCl_3 . Both the high-contrast pattern and the appearance of thiol groups support the spatially-controlled reduction of disulfides into thiols (Figure 2D). This strategy also enabled the fabrication of a wettability gradient on the surface as shown in the Supporting Information, Figure S16.

These two photochemical reactions, UV-DF and UV-DR, allow for reversible transitions between thiol-functionalized surfaces and disulfide-functionalized surfaces. To evaluate this reversibility, we sequentially modified a thiol-functionalized film through the UV-DF reaction with BDS, followed by the UV-DR reaction with DTT (Figure 3A). After exchange with BDS, this hydrophilic surface becomes hydrophobic, as observed in the increasing static WCA from $54 \pm 2^\circ$ to $118 \pm 2^\circ$; subsequent UV-DR reaction restores the original hydrophilic surface with a static WCA of $54 \pm 2^\circ$. The transforma-

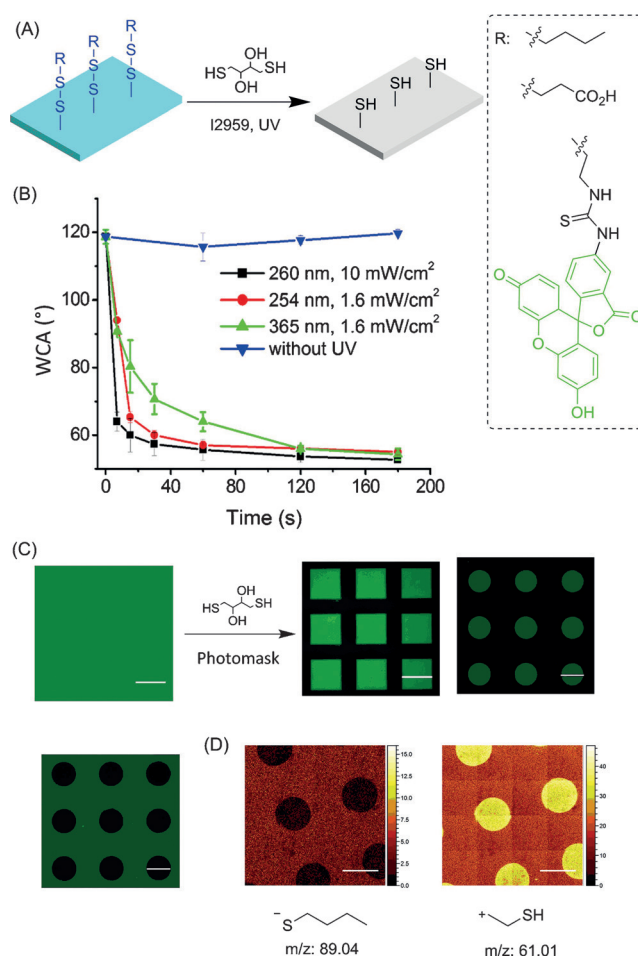


Figure 2. A) Representation of the UV-DR reaction on disulfide-modified surfaces. B) Rate of surface modification by the UV-DR reaction in DMF. The graph shows the static WCA on BDS-modified surface after the UV-DR reaction as a function of irradiation time under different UV radiation sources. C) Fluorescence microscopy image of (FITC-disulfide)-modified surfaces before and after patterning by using the UV-DR reaction through different photomasks. Scale bar = 500 μm . D) ToF-SIMS images of (dibutyl disulfide)-modified surface patterned by using the UV-DR reaction. Scale bar = 500 μm .

tion between hydrophilic and hydrophobic surfaces is very quick as every step needs only 2 min of UV irradiation. SEM measurements revealed no change of surface topography after the UV-DR and UV-DF reactions (Figure 3B,C). This process can be repeated for at least ten cycles, which demonstrates good reversibility (Figure 3D). The slight decrease of static WCA for both surfaces possibly results from oxidation of thiol groups or disulfide groups over time and under UV light. After ten cycles, the thiol concentration on this surface was $1.64 \times 10^{-9} \text{ mol mm}^{-2}$, which corresponds to 85 % of intact thiols.

Reversible UV-induced disulfide formation and reduction offer unique opportunities for dynamic photopatterning. Additionally, as the disulfide-modified surface produced is photodynamic itself, it opens the possibility for photodynamic disulfide exchange using other disulfides.^[13] Therefore, we can use light to direct the attachment, exchange, and detachment of moieties immobilized through the disulfide bond with

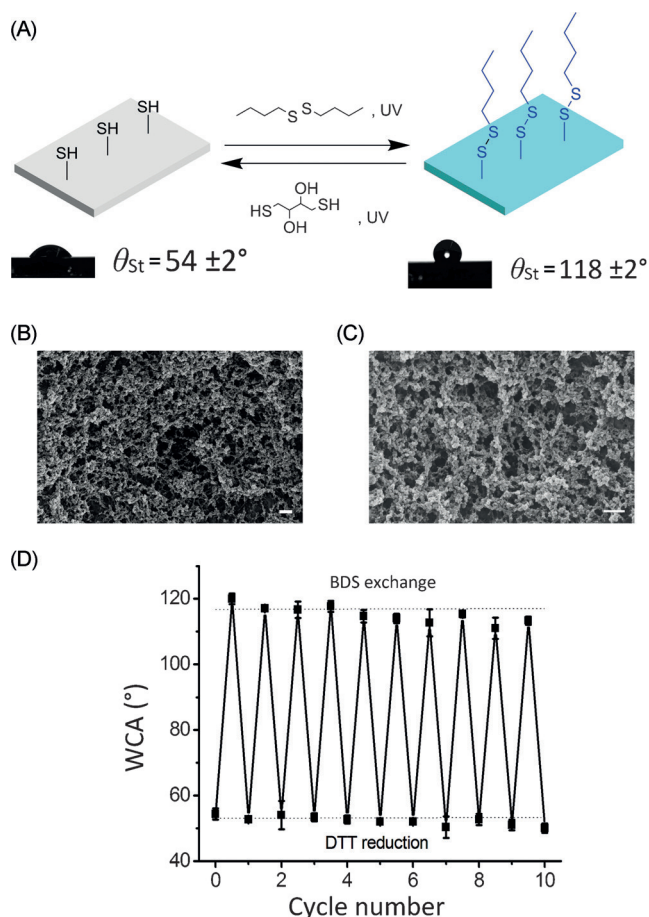


Figure 3. Reversible surface modification based on UV-DF and UV-DR reactions. A) Representation of the change of surface wettability by using the UV-DF reaction with dibutyl disulfide and the UV-DR reaction in DMF. SEM images showing the porous structures of a B) thiol-modified surface and a C) (dibutyl disulfide)-modified surface. Scale bar = 300 nm. D) The reversible process was repeated ten times, and the static WCA of the surface was measured after each modification.

spatial and temporal control (Scheme 1). This dynamic photopatterning has been demonstrated with dansyl disulfide (DDS; Figure 4A). By using the UV-DF, DDS was attached onto a thiol-functionalized film, producing the dansyl fluorescence image in Figure 4B. The PDDE reaction permits the exchange between immobilized DDS and the nonfluorescent BDS with spatial control, demonstrated by the disappearance of dansyl fluorescence in the exposed regions (Figure 4C). Finally, the detachment process was confirmed by the disappearance of the dansyl pattern after the UV-DR reaction (Figure 4D). This strategy possesses the living nature for surface photopatterning, allowing multiple and reversible manipulations of surface properties using light. This possibility has been demonstrated by the second attachment, exchange, and detachment of DDS on the regenerated thiol-modified surface (Figure 4E–G).

This study demonstrates the UV-induced disulfide formation and reduction reactions for surface functionalization and dynamic photopatterning, which permits the light-induced attachment, exchange, and detachment of surface functional groups. In this work, UV light was used to

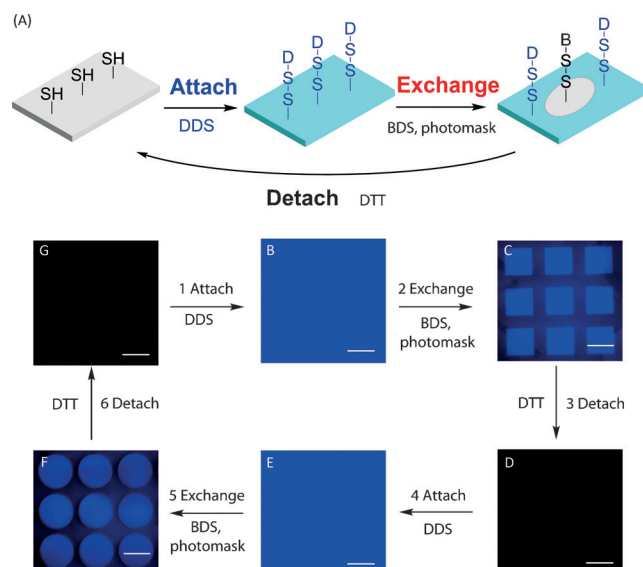


Figure 4. Dynamic photopatterning allows reversible attachment, exchange, and detachment of disulfide-bonded substrates on the surface. A) Representation of UV-induced attachment of dansyl disulfide (DDS), exchange between DDS and dibutyl disulfide (BDS) using a photomask, and detachment of disulfide molecules. Fluorescence microscopy images of a thiol-modified surface after the following sequential treatment: B) Flood irradiation in the presence of DDS, C) masked irradiation with BDS, D) flood irradiation with DTT, E) flood irradiation with DDS, F) masked irradiation with BDS, and G) flood irradiation with DTT. Scale bar = 500 μm .

demonstrate these possibilities; however, visible light and even NIR light can also be used to trigger these reactions through the rational selection of photoinitiators. We foresee that this photodynamic thiol–disulfide exchange process and dynamic photopatterning strategy will provide a new tool for the precise manipulation of interfacial properties and the development of stimulus-responsive surfaces and new smart materials.

Acknowledgements

The research was supported by the Helmholtz Association's Initiative and Networking Fund (grant VH-NG-621) and the European Research Council starting grant (ERC-2013-StG 337077-DropCellArray).

Keywords: disulfide formation · disulfide reduction · dynamic photopatterning · photochemistry · surface modification

How to cite: *Angew. Chem. Int. Ed.* **2016**, 55, 13765–13769
Angew. Chem. **2016**, 128, 13969–13973

- [1] P. K. Sorger, *Nat. Biotechnol.* **2008**, 26, 1345–1346.
- [2] T. B. Singh, N. S. Sariciftci, *Annu. Rev. Mater. Res.* **2006**, 36, 199–230.
- [3] X. Yao, R. Peng, J. Ding, *Adv. Mater.* **2013**, 25, 5257–5286; R. Ogaki, M. Alexander, P. Kingshott, *Mater. Today* **2010**, 13, 22–

- 35; X. Deng, C. Friedmann, J. Lahann, *Angew. Chem. Int. Ed.* **2011**, *50*, 6522–6526; *Angew. Chem.* **2011**, *123*, 6652–6656.
- [4] G. Delaittre, A. S. Goldmann, J. O. Mueller, C. Barner-Kowollik, *Angew. Chem. Int. Ed.* **2015**, *54*, 11388–11403; *Angew. Chem.* **2015**, *127*, 11548–11564; S. Petersen, J. M. Alonso, A. Specht, P. Duodu, M. Goeldner, A. del Campo, *Angew. Chem. Int. Ed.* **2008**, *47*, 3192–3195; *Angew. Chem.* **2008**, *120*, 3236–3239; J. Cui, V. S. Miguel, A. del Campo, *Macromol. Rapid Commun.* **2013**, *34*, 310–329.
- [5] C. A. DeForest, B. D. Polizzotti, K. S. Anseth, *Nat. Mater.* **2009**, *8*, 659–664.
- [6] R. M. Hensarling, V. A. Doughty, J. W. Chan, D. L. Patton, *J. Am. Chem. Soc.* **2009**, *131*, 14673–14675.
- [7] B. J. Adzima, Y. Tao, C. J. Kloxin, C. A. DeForest, K. S. Anseth, C. N. Bowman, *Nat. Chem.* **2011**, *3*, 256–259.
- [8] R. K. V. Lim, Q. Lin, *Acc. Chem. Res.* **2011**, *44*, 828–839.
- [9] W. Feng, L. Li, C. Yang, A. Welle, O. Trapp, P. A. Levkin, *Angew. Chem. Int. Ed.* **2015**, *54*, 8732–8735; *Angew. Chem.* **2015**, *127*, 8856–8859.
- [10] S. Arumugam, V. V. Popik, *J. Am. Chem. Soc.* **2011**, *133*, 15730–15736.
- [11] S. Arumugam, V. V. Popik, *J. Am. Chem. Soc.* **2012**, *134*, 8408–8411.
- [12] N. R. Gandavarapu, M. A. Azagarsamy, K. S. Anseth, *Adv. Mater.* **2014**, *26*, 2521–2526.
- [13] X. Du, J. Li, A. Welle, L. Li, W. Feng, P. A. Levkin, *Adv. Mater.* **2015**, *27*, 4997–5001.
- [14] R. P. Szajewski, G. M. Whitesides, *J. Am. Chem. Soc.* **1980**, *102*, 2011–2026.
- [15] Y. Amamoto, H. Otsuka, A. Takahara, K. Matyjaszewski, *Adv. Mater.* **2012**, *24*, 3975–3980; J. Li, J. M. A. Carnall, M. C. A. Stuart, S. Otto, *Angew. Chem. Int. Ed.* **2011**, *50*, 8384–8386; *Angew. Chem.* **2011**, *123*, 8534–8536; H. Otsuka, S. Nagano, Y. Kobashi, T. Maeda, A. Takahara, *Chem. Commun.* **2010**, *46*, 1150–1152; B. D. Fairbanks, S. P. Singh, C. N. Bowman, K. S. Anseth, *Macromolecules* **2011**, *44*, 2444–2450.
- [16] L. Wang, L. Li, X. Wang, D. Huang, F. Yang, H. Shen, Z. Li, D. Wu, *Polym. Chem.* **2016**, *7*, 1429–1438.
- [17] F. L. Geyer, E. Ueda, U. Liebel, N. Grau, P. A. Levkin, *Angew. Chem. Int. Ed.* **2011**, *50*, 8424–8427; *Angew. Chem.* **2011**, *123*, 8575–8578.
- [18] K. Brocklehurst, J. Carlsson, M. P. J. Kierstan, E. M. Crook, *Biochem. J.* **1973**, *133*, 573–584; V. Grazú, O. Abian, C. Mateo, F. Batista-Viera, R. Fernández-Lafuente, J. M. Guisán, *Biomacromolecules* **2003**, *4*, 1495–1501.
- [19] W. W. Cleland, *Biochemistry* **1964**, *3*, 480–482.

Received: July 27, 2016

Revised: September 3, 2016

Published online: October 4, 2016